RESEARCH ARTICLE
PLANETARY SCIENCES

Earth and Planetary Physics
9: 1099–1112, 2025
doi: 10.26464/epp2025085

Classification and provenance of exotic impact glasses in Chang'e-5 lunar soil

YunHong Fan[1,2], BiWen Wang[2,3], Wei Yang[1*], QiuLi Li[3], HuiJuan Zhang[4], and ShiTou Wu[3]

[1]Key Laboratory of Earth and Planetary Physics, Institute of Geology and Geophysics, Chinese Academy of Sciences, Beijing 100029, China;

[2]College of Earth and Planetary Sciences, University of Chinese Academy of Sciences, Beijing 100049, China;

[3]State Key Laboratory of Lithospheric Evolution, Institute of Geology and Geophysics, Chinese Academy of Sciences, Beijing 100029, China;

[4]East China University of Technology, Nanchang 330013, China

Key Points:

- We selected 28 impact glasses with "exotic" major element compositions from Chang'e-5 soil for trace element analysis.
- Eighteen of the analyzed glasses exhibited trace element compositions comparable to those of the local Chang'e-5 materials.
- We propose a new plot, La versus Mg#, for distinguishing between local and exotic impact glasses in Chang'e-5 soil.

Citation: Fan, Y. H., Wang, B. W., Yang, W., Li, Q. L., Zhang, H. J., and Wu, S. T. (2025). Classification and provenance of exotic impact glasses in Chang'e-5 lunar soil. *Earth Planet. Phys.*, *9*(6), 1099–1112. http://doi.org/10.26464/epp2025085

Abstract: Lunar impact glasses have been identified as crucial indicators of geochemical information regarding their source regions. Impact glasses can be categorized as either local or exotic. Those preserving geochemical signatures matching local lithologies (e.g., mare basalts or their single minerals) or regolith bulk soil compositions are classified as "local". Otherwise, they could be defined as "exotic". The analysis of exotic glasses provides the opportunity to explore previously unsampled lunar areas. This study focuses on the identification of exotic glasses within the Chang'e-5 (CE-5) soil sample by analyzing the trace elements of 28 impact glasses with distinct major element compositions in comparison with the CE-5 bulk soil. However, the results indicate that 18 of the analyzed glasses exhibit trace element compositions comparable to those of the local CE-5 materials. In particular, some of them could match the local single mineral component in major and trace elements, suggesting a local origin. Therefore, it is recommended that the investigation be expanded from using major elements to including nonvolatile trace elements, with a view to enhancing our understanding on the provenance of lunar impact glasses. To achieve a more accurate identification of exotic glasses within the CE-5 soil sample, a novel classification plot of Mg# versus La is proposed. The remaining 10 glasses, which exhibit diverse trace element variations, were identified as exotic. A comparative analysis of their chemical characteristics with remote sensing data indicates that they may have originated from the Aristarchus, Mairan, Sharp, or Pythagoras craters. This study elucidates the classification and possible provenance of exotic materials within the CE-5 soil sample, thereby providing constraints for the enhanced identification of local and exotic components at the CE-5 landing site.

Keywords: Chang'e-5; impact glass; exotic materials; classification; provenance

1. Introduction

Lunar impact glasses are common in lunar soils, which may be formed by impact melting of local materials or transportation of materials from distant impact craters (Zellner, 2019). The ratios of refractory elements remain unaffected by volatile losses (Delano et al., 1981, 2007), thereby offering significant insights into the lunar surface composition (Meyer, 1978; Korotev et al., 2010). The impact glasses exhibit compositions distinct from the local geological units, suggesting either exotic origins or the presence of unidentified underlying geological formations (Rhodes et al., 1977; Zellner et al., 2002; Zeigler et al., 2006; Wu YH et al., 2023). As a result, the study of these exotic impact glasses contributes to our understanding of the lunar surface. Further geochemical investigations can provide insights into the history, processes, and magnitudes of lunar impact events (Zellner, 2019). Therefore, the identification and provenance of these exotic glasses are crucial for advancing our knowledge of the distribution and transportation of materials on the lunar surface.

Prior studies have identified a multitude of exotic glasses in the Apollo samples. For example, Delano et al. (2007) utilized a ternary diagram of titanium (Ti), magnesium (Mg), and aluminum (Al) to analyze soil samples 60014, 64501,225, and 66041, 127 from Apollo 16. The results demonstrated that approximately 30% of the sample population consisted of exotic compositions, constituted as determined by the ratio of nonvolatile lithophilic

First author: Y. H. Fan, yhfan@mail.iggcas.ac.cn
Correspondence to: W. Yang, yangw@mail.iggcas.ac.cn
Received 10 DEC 2024; Accepted 08 APR 2025.
First Published online 09 JUL 2025.

elements to elucidate the origins of the impact glasses. Korotev et al. (2010) used a variety of diagrams to differentiate between glass groups, including mare and nonmare types. Norman et al. (2019) examined major and trace elements in 30 glasses from Apollo 16 soil sample 66031. The analysis revealed a diverse range of chemical compositions, with ~50% of the glasses falling into the category of "exotic." The remaining glasses display similarities to the local Apollo 16 soils, which have been classified as "local." These findings have substantially enhanced our understanding of the mechanisms by which materials are transported on the lunar surface.

Forty-four years after the Apollo and Lunar missions, the Chang'e-5 (CE-5) mission has successfully collected lunar samples from one of the youngest lunar mare basalt units (~2.0 Ga) located in the northern region of Oceanus Procellarum (Che XC et al., 2021; Li QL et al., 2021; Hao JL et al., 2024). These samples may encompass a variety of crustal components from distant regions that were transported to the CE-5 landing site by impact events (Qian YQ et al., 2021). These exotic materials were defined as those exhibiting distinct major and trace element compositions relative to the surface regolith of the landing site, local basaltic materials, and local selective melt components, including mare basalt, bulk soil, and single minerals (Yang W et al., 2022; Zeng XJ et al., 2022; Chen Y et al., 2023; Mei AX et al., 2023; Wu YH et al., 2023). For example, the exotic impact glasses present in the CE-5 samples offer a valuable opportunity to investigate materials not directly sampled by the mission. The chemical compositions of the impact glasses have been analyzed with the objective of identifying their provenance (Yang W et al., 2022; Long T et al., 2022). However, Wu YH et al. (2023) found that some glasses in the CE-5 soil exhibit chemical compositions distinct from the bulk soil and concluded that these glasses should not be classified as exotic. The observed chemical variations could be attributed to impact-induced crushing, differential crystallization, impact melting, and volatilization (Wu YH et al., 2023; Yan P et al., 2024). This result indicates that the proportion of exotic materials may be lower than previously assumed. It is necessary to integrate multi-elemental analytical approaches spanning both major and trace element systems to establish a robust classification of the CE-5 impact glasses.

To enhance our comprehension of the exotic glasses identified in the CE-5 soils, we conducted a preliminary classification based on the major element compositions of a data set comprising 764 glasses (Wang BW et al., 2024). From this data set, 28 glasses exhibiting major element characteristics distinct from those of the CE-5 basalt were selected for laser ablation inductively coupled plasma mass spectrometry (LA-ICP-MS) analyses. Our results provide critical constraints for the precise identification of local and exotic components at the CE-5 landing site.

2. Samples and Methods

The investigation was primarily focused on a selection of 764 impact glasses, which had previously been examined by Wang BW et al. (2024). The lunar soil samples were obtained from the China National Space Administration under a materials transfer agreement. We used one scooped sample (CE5C0600YJFM, from which the three volcanic glass beads were extracted) and three drilled samples (CE5Z0107YJFM, CE5Z0303YJFM, and CE5Z0403YJFM). From a comparative analysis of the major elemental compositions with an electron probe microanalyzer (EPMA; Wang BW et al., 2024; Figure 1) and CIPW (the method proposed by Cross, Iddings, Pirsson, and Washington, who used this acronym as the name of their calculation method) normative data (Table S4), we selected 28 glasses that exhibited distinct major element characteristics in comparison with the CE-5 bulk soil for trace element analyses. The backscattered electron (BSE) images of the selected glasses are displayed in Figure S1. As can be seen in these images, and as described in Wang BW et al. (2024), some of these glasses are clean glasses (e.g., 38-3, 44-4, 45-41, 50-50), and some glasses do contain schlieren (e.g., 51-201), vesicles (e.g., 50-107), FeNi metal (e.g., 39-277), and rims of adhering regolith (e.g., 49-39).

Trace element analyses were conducted by LA-ICP-MS at the Institute of Geology and Geophysics, Chinese Academy of Sciences (IGGCAS). This technique is particularly advantageous for analyzing

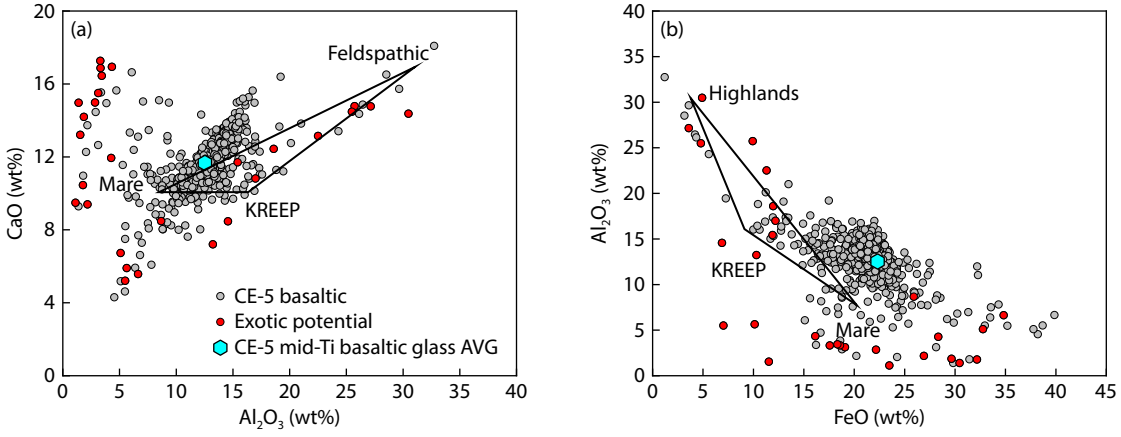

Figure 1. CaO versus Al_2O_3 and Al_2O_3 versus FeO of selected glasses in major elements using an EPMA (Wang BW et al., 2024). The red dots represent the glasses, which have major element compositions that are distinct from those of the CE-5 basalt. The data on CE-5 mid-Ti basaltic glass are from Yang W et al. (2022). The highlands, feldspathic, KREEP (samples rich in potassium, rare earth elements, and phosphorus), and mare compositions are from Lucey (2006). AVG, average.

the bulk composition of glasses, as opposed to the limited source diameter characteristic of the EPMA. The Element XR HR-ICP-MS instrument was coupled to a 193 nm ArF excimer laser system (GeoLas HD). The laser has a diameter of approximately 16 μm with a repetition rate of 5 Hz. We used ARM-1 (Wu ST et al., 2019) reference glass for external calibration, and NIST (National Institute of Standards and Technology) SRM (Standard Reference Material) 610 (Jochum et al., 2011) and U.S. Geological Survey BCR-2G (microanalysis glass, Columbia River Basalt; Jochum et al., 2005) glasses for quality control monitoring. The bulk normalization to 100 wt% strategy was used for data reduction, using the Iolite software package with an in-house-built DRS (Data Reduction Scheme) code (Wu ST et al., 2018). For most trace elements (>0.5 ppm), the 2SE represents 2 standard error for each point of internal precision (Table S2), and the accuracy is better than ±20% (Wu ST et al., 2019). The data on glasses and references are listed in Tables S1 and S3, along with the error values listed in Table S2. The major elements and the results of CIPW are listed in Table S4. We calculated the average as the bulk composition when the glass was measured multiple times. Therefore, the compositional data presented in this study can represent bulk glass compositions.

3. Results

The chemical compositions of impact glasses are indicative of their original target materials. In particular, the ratios of refractory elements remain unaffected by volatile losses (Delano et al., 1981, 2007). In this study, the classification methodology places particular emphasis on refractory elements such as Al_2O_3, FeO, MgO, CaO, and rare earth elements (REEs). The selected glasses can be divided according to the major and trace elements analyzed by LA-ICP-MS into two main groups: (1) local glass and (2) exotic glass (see Figures 2 and 3, Tables 1 and 2).

3.1 Local Glass

A total of 18 glasses were classified as of local origin, based on the data obtained from trace elements. The local glasses exhibit three distinct chemical compositions: basaltic, single mineral, and mixture glass.

The four basaltic glasses, 49-151, 51-124, 51-132, and 51-215, exhibit notable variations in major element compositions when compared with the CE-5 bulk soil (Table 1). These variations are evident in the TiO_2 (2.91–4.15 wt%), FeO (16.74–29.50 wt%), CaO (9.57–12.00 wt%), and MgO (4.83–8.41 wt%) contents. However, they exhibit Mg# (~23–45, Mg# = molar Mg/(Mg + Fe) × 100) and

Table 1. Chemical composition of local glasses.

Sample No.	49-151	51-124	51-132	51-215	45-97	49-59	51-101	51-201	51-242	48-110	41-164	43-276	47-134 (avg.)[a]	49-39	49-207	50-107	51-73	51-164
(wt%)																		
SiO_2	43.9	45.9	47.63	46.3	48.16	46.69	49.8	49.41	50.9	47.3	49.54	48.48	35.12	46.11	48.50	35.41	60.1	46.42
TiO_2	4.15	3.46	2.91	3.55	2.28	1.05	1.14	1.09	1.89	0.11	0.87	1.61	15.55	2.61	4.14	13.47	2.50	4.01
Al_2O_3	4.07	11.16	13.83	12.44	3.02	1.38	8.70	1.28	4.80	32.6	20.2	3.07	7.66	7.51	12.8	8.29	10.61	8.6
FeO	29.5	18.8	16.74	18.2	18.28	29.32	19.89	31.67	19	1.28	7.1	25.27	25.51	25.40	18.8	30.35	13.3	21.6
MnO	0.34	0.22	0.19	0.2	0.26	0.36	0.28	0.39	0.28	0.02	0.11	0.35	0.24	0.3	0.25	0.29	0.15	0.25
MgO	4.83	5.3	6.72	8.41	10.55	3.95	7.82	5.76	10.55	0.39	4.91	8.48	6.16	5.20	7.55	5.04	5.79	9.08
CaO	11.88	12	10.67	9.57	17.24	16.79	11.7	10.21	13	17	15.94	12.36	8.97	12.04	8.1	6.37	6	9.02
Na_2O	0.11	0.55	0.45	0.54	n.d.	n.d.	0.44	0.03	0.25	1.16	0.86	0.06	0.11	0.29	n.d.	0.19	0.5	0.3
K_2O	0.10	0.4	0.24	0.18	n.d.	0.02	0.08	0	0.06	0.07	0.08	0.13	0.11	0.08	0.42	0.07	0.29	0.17
P_2O_5	0.27	1.64	0.18	0.23	n.d.	0.05	0.02	0.02	0.13	n.d	0.1	0.16	0.11	0.10	n.d.	0.13	0.38	0.21
(ppm)																		
Li	0	13	16	n.d.	3	n.d.	3	3	0	20	4	9	15	n.d.	n.d.	13	37	5
B	28	69	6	30	n.d.	25	13	3	10	n.d.	15	13	22.4	19	12	4	n.d.	26
Sc	100	86	48.1	37.9	159	173	78.9	134	71	0.2	105	118	65.7	88	121	30.7	29	52.4
V	98	121	58	76	244	73	60.4	52.9	74.6	5.5	143	78.5	131	78.4	151	77.3	40	73.3
Cr	1052	1460	1277	1395	2180	1410	582	536	1185	40	1310	732	1920	1330	1850	1342	790	1313
Co	49	23.7	32.2	41.3	35.2	25.7	31.9	40.8	39.9	2.6	19	33.7	33.7	32.9	35.4	27.1	36	38.8
Ni	60	131	227	253	16	n.d.	23	12	45	32	n.d.	6	89	97	135	50	190	124
Cu	97	10	4.3	21.9	n.d.	n.d.	1	4.9	n.d.	6.8	3.7	5.7	n.d.	3	n.d.	7.7	15	12.1
Zn	n.d.	1	4	34	n.d.	n.d.	n.d.	n.d.	10	n.d.	n.d.	1	27.5	3	4	29	62	22
Ga	5	4.8	4.7	4.9	2.9	8	2.8	1.7	0.35	11.8	4.9	4.4	3.9	5.2	3.8	3.5	1.8	3.4
Rb	1.81	5.8	4.2	5.1	0.29	0.16	0.74	0.04	1.84	0.99	0.55	3.1	1.78	1.5	1.4	5	7.6	1.65
Sr	137	279	256	266	24.7	70.8	194	17	48	533	277	120	167	174	206	177	311	213

Continued from Table 1

Sample No.	49-151	51-124	51-132	51-215	45-97	49-59	51-101	51-201	51-242	48-110	41-164	43-276	47-134 (avg.)[a]	49-39	49-207	50-107	51-73	51-164
Y	104	114	114	84	51.7	186	38.4	52	34.1	0.38	27.1	74	58.5	75.6	75.9	73.4	35	61.9
Zr	395	528	506	225	89.9	683	64.4	70.7	118	n.d.	83	274	517	230	281	480	164	272
Nb	29.9	49.6	31.9	22.8	0.11	0.73	1.44	0.3	6.2	0.19	3.8	12.9	48.5	12	17.3	43.7	16.2	24.7
Cs	0.17	0.69	15	127	0.05	0.04	0.07	0.08	0.27	n.d.	0.02	0.04	0.1	0.24	0.07	1.08	1.36	0.16
Ba	171	540	457	265	n.d.	1.7	55.6	1.4	141	71	76	235	224	167	200	255	331	218
La	29.5	35.9	37.3	32.5	1.37	7.79	3.51	1.93	6.8	0.77	5.5	21.4	18.4	15.8	22	23.8	19.5	21.3
Ce	75.5	94	90.2	81	9.3	36.1	10.3	7	17	2.4	12.6	53	44.6	36.7	58	64.1	50	51
Pr	11.8	13.4	14.7	11.2	2.32	7.15	2.46	1.55	2.4	n.d.	2.43	7.7	6.01	5.6	8.1	8.5	6.6	7
Nd	57	59	62	44.5	15.9	45.2	10.9	10.4	7.5	1.7	10	34	28	28.4	48	43.9	20.5	34.9
Sm	16.1	23	17.8	15	5.5	15.8	4.8	5.3	5.4	0.89	3.5	9.4	9.25	7.8	13.5	12	5	8.2
Eu	1.1	1.57	2.7	2.4	0.46	1.78	0.71	0.27	0.21	2.9	1.91	1.15	1.81	1.81	1.19	1.64	4	2.14
Gd	17.5	29.7	19.2	13.8	8.1	27.1	6.6	6.8	6.2	1.7	7.4	12.2	10.5	15.3	15.6	15.6	4.8	14.5
Tb	3.27	3.14	3.05	3.09	1.68	5.57	0.78	1.39	1.62	0.04	n.d.	2.2	1.75	2.92	2.82	2.49	n.d.	2.27
Dy	22.7	18.5	23	15.4	9.6	39.7	7.2	10.4	4.6	n.d.	7.4	15	11.7	17.7	19.5	13.6	n.d.	13.4
Ho	4.11	6.38	4.29	3.55	1.95	7.59	1.93	2.24	1.58	0.23	1.3	2.7	2.66	3.46	3.15	3.45	1.3	2.49
Er	10.2	11.3	12	9.2	4.5	23	4.5	5.9	5.2	n.d.	n.d.	7.2	6.7	9	7.7	8.9	3.2	7.1
Tm	1.6	2.1	1.58	1.41	0.7	3.86	0.7	0.82	0.57	n.d.	0.5	0.92	1.15	1.19	1.21	1.19	0.51	0.89
Yb	9.5	21.4	11	5.6	3.8	22	5.2	5.9	4.3	n.d.	n.d.	6.4	7.2	5.7	5.9	8.3	4	5.3
Lu	1.36	0.81	1.27	0.98	0.62	3.89	0.77	0.77	1.35	0.08	0.62	1.05	1.06	0.87	0.44	1.22	0.4	1.03
Hf	10.2	16.4	16.7	6.1	5	32.3	2.57	2.65	1.9	0.07	1.79	7.4	13.4	5.7	11.1	11.9	5.5	8.8
Ta	1.33	3.3	1.62	0.73	0.07	0.08	n.d.	0.02	0.31	0.15	0.31	0.75	3.14	0.42	0.91	2.59	1.4	1.15
Pb	0.87	0.81	0.85	1.47	n.d.	0.02	0.07	0.13	0.32	0.03	0.15	0.54	0.33	1.1	0.16	0.19	1.6	0.37
Th	2.64	3.79	4.98	4.8	n.d.	0.44	0.28	n.d.	0.76	n.d.	1.04	2.5	2.68	1.86	2.46	3.63	1.8	2.8
U	0.67	1.16	1.34	0.51	n.d.	0.14	0.03	n.d.	0.04	n.d.	0.34	0.69	0.82	0.72	0.44	1.2	0.78	0.44
Zr/Y	3.79	4.63	4.44	2.68	1.74	3.67	1.68	1.36	3.46		3.06	3.7	8.85	3.04	3.7	6.54	4.69	4.39
Sc/Sm	6.21	3.74	2.7	2.53	29.0	11.0	16.4	25.3	13.2	0.22	30.0	12.6	7.1	11.3	8.96	2.56	5.8	6.39
$(Eu/Eu^*)_N$	0.2	0.18	0.45	0.51	0.21	0.26	0.38	0.14	0.11	7.19	1.14	0.33	0.56	0.51	0.25	0.37	2.49	0.6
$(Sm/Yb)_N$	1.84	1.17	1.76	2.91	1.57	0.78	1	0.98	1.37			1.6	1.4	1.49	2.49	1.57	1.36	1.68
$(La/Yb)_N$	2.11	1.14	2.3	3.94	0.24	0.24	0.46	0.22	1.07			2.27	1.74	1.88	2.53	1.95	3.31	2.73

[a]avg., average.

REE concentrations similar to those of the CE-5 basalt (Figure 4a), showing an enrichment in light REEs (LREEs) and a depletion in heavy REEs (HREEs).

Five glasses were identified as pyroxene-like. They exhibit low Al_2O_3 (<5 wt%; Table 1), higher FeO, and lower MgO contents than the highland pyroxene. Their compositions fall within the CE-5 pyroxene fields on the MgO versus FeO and FeO versus Al_2O_3 diagrams (Figure 2). With regard to trace elements, they are characterized by an obvious negative Eu anomaly (Table 1), accompanied by a depletion in LREEs (Figure 4b), consistent with those pyroxenes in the CE-5 basalt (Figure 4b). One glass (51-101) exhibits higher Al_2O_3 (8.70 wt%) than the other four glasses, and its major element characteristics are similar with low-Ti basalt/regolith (Maxwell and Wiik, 1971; Wakita et al., 1971; Helmke et al., 1973; Snyder et al., 1997). However, this glass has enriched HREEs, with lower $(La/Lu)_N$ and $(La/Yb)_N$ ratios (<1; Table S1). Conversely, the low-Ti basalt/regolith has these two ratios >1 (Maxwell and Wiik, 1971; Wakita et al., 1971; Helmke et al., 1973; Snyder et al., 1997).

One glass (48-110) was identified as plagioclase-like, which exhibits high Al_2O_3 (32.60 wt%) and CaO (17.00 wt%) contents and a low FeO content (1.28 wt%) with an obvious Eu-positive anomaly in the REE patterns (Figure 4c). These characteristics are similar to those of the lunar highland anorthosites (Figure S2). However, the chemical composition of this glass is similar to that of the plagioclase in the CE-5 basalt with regard to CaO, FeO, MgO, and Al_2O_3 contents (Figure 3). The higher FeO and lower CaO contents are distinct from highland plagioclases (Figures 3a, 3c, and 3d). The REE analysis revealed that the sample contains an REE concentration similar to the plagioclases in the CE-5 basalt.

Eight glasses, namely 41-164, 43-276, 47-134, 49-39, 49-207, 50-107, 51-73, and 51-164, exhibit mixing features of local materials. Their major elements display a wide range (Table 1), for example, in the TiO_2 (4.01–15.55 wt%), Al_2O_3 (7.51–12.80 wt%), and FeO (18.80–30.35 wt%) contents (Table 1). We utilized a geochemical modeling approach similar to that proposed by Korotev et al. (1995), based on the local mineral assemblages (e.g., pyroxene and plagioclase) and the bulk compositions of major elements and REE from the CE-5 basalt (Tian HC et al., 2021; Chen Y et al., 2023). The objective of the model calculations was to satisfy both the major and trace element data simultaneously (see Table S5). For example, glass 50-107 can be formed by a mixture of 70% CE-

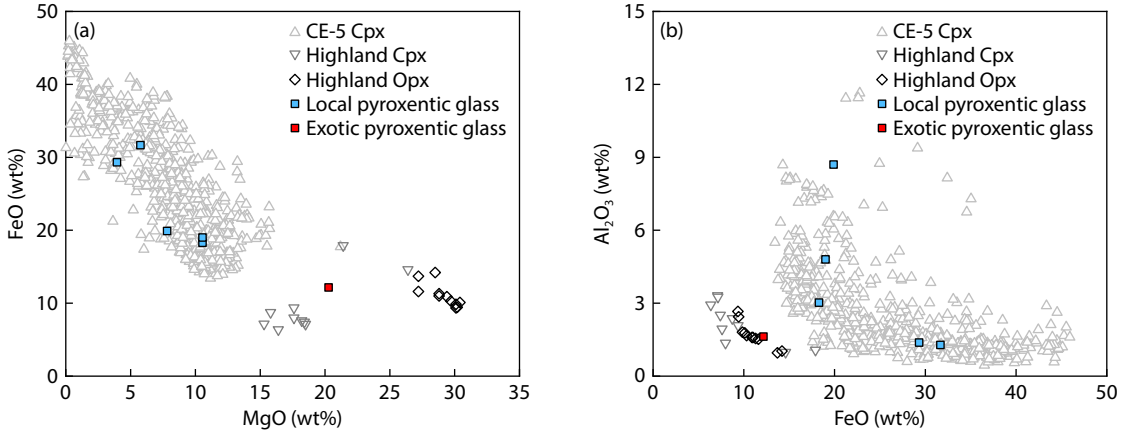

Figure 2. Major elements of pyroxenitic glasses compared with the CE-5 and highland composition of pyroxene. One glass was near highland pyroxene. The data on CE-5 pyroxene are from Tian HC et al. (2021), and the data on highland samples are from Floss et al. (1998). Cpx, clinopyroxene; Opx, orthopyroxene.

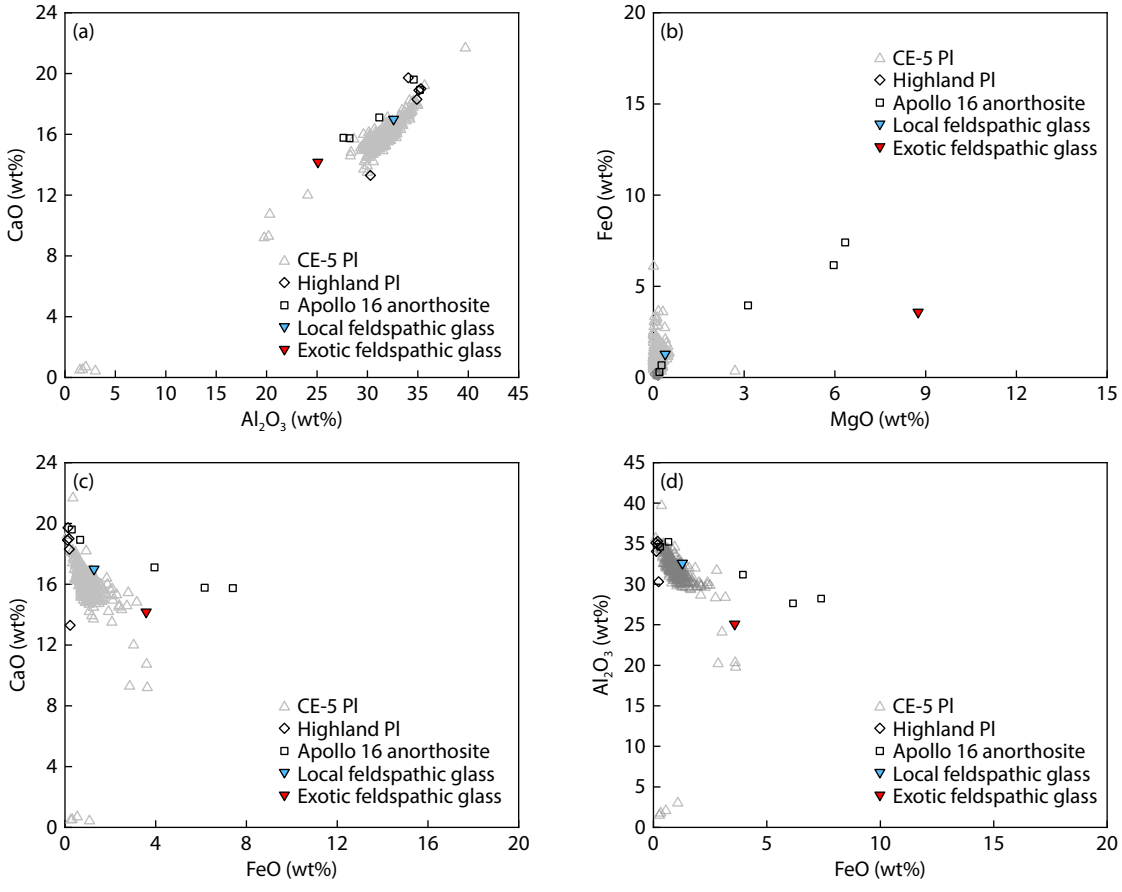

Figure 3. Major elements of feldspathic glass compared with the plagioclase of the CE-5 basalt and Apollo 16 anorthosite samples. Data on the CE-5 plagioclase are from Che XC et al. (2021), Hu S et al. (2021), Jiang Y et al. (2022), Tian HC et al. (2021), and He Q et al. (2022). Data on the Apollo 16 anorthosite plagioclase are from Rose et al. (1973), Dymek et al. (1975), Powell et al. (1975), Wänke et al. (1975), Dominik and Jessberger (1978), Ryder and Norman (1980), Papike et al. (1997), and Norman et al. (2003). Pl, plagioclase.

5 basalt and 30% ilmenite (see Figure 4d and Table S5), whereas glass 43-276 can be formed by a mixture of 55% CE-5 basalt and 45% pyroxene (see Figure 4e and Table S5). In total, these glasses can be formed by mixing 40–75 wt% CE-5 basalt with 25–60 wt% single minerals (clinopyroxene, plagioclase, and ilmenite from the CE-5 basalt; see Table S5 for details).

3.2 Exotic Glass

The remaining 10 glasses were identified as exotic glass. They exhibit a wide range of chemical characteristics (see Figures 5 and 6).

One glass, 38-3, has a noritic composition with a high Al_2O_3 content (23.95 wt%; Table 2), a slight Eu-negative anomaly ($(Eu/Eu^*)_N = 0.6$), and a high Mg# (73; Table 2). The REE concentrations in this glass are lower than those observed in the Apollo noritic samples (e.g., noritic matrix 15455; Taylor et al., 1972; Figure 6a). The CIPW normative results indicated that the glass is composed of 67.35 wt% plagioclase and 25.79 wt% hypersthene (Table S4). Two glasses, 45-41 and 51-232, exhibit similarities with the KREEP (samples rich in potassium, REEs, and phosphorus) basalts in terms of major element compositions, including low FeO and high Al_2O_3 contents. It is noteworthy that there are considerable enrichments in incompatible trace elements, particularly Th concentrations (Table 2). Another glass, 41-101, presents high TiO_2 (8.18 wt%) and FeO (17.60 wt%) contents with a depletion

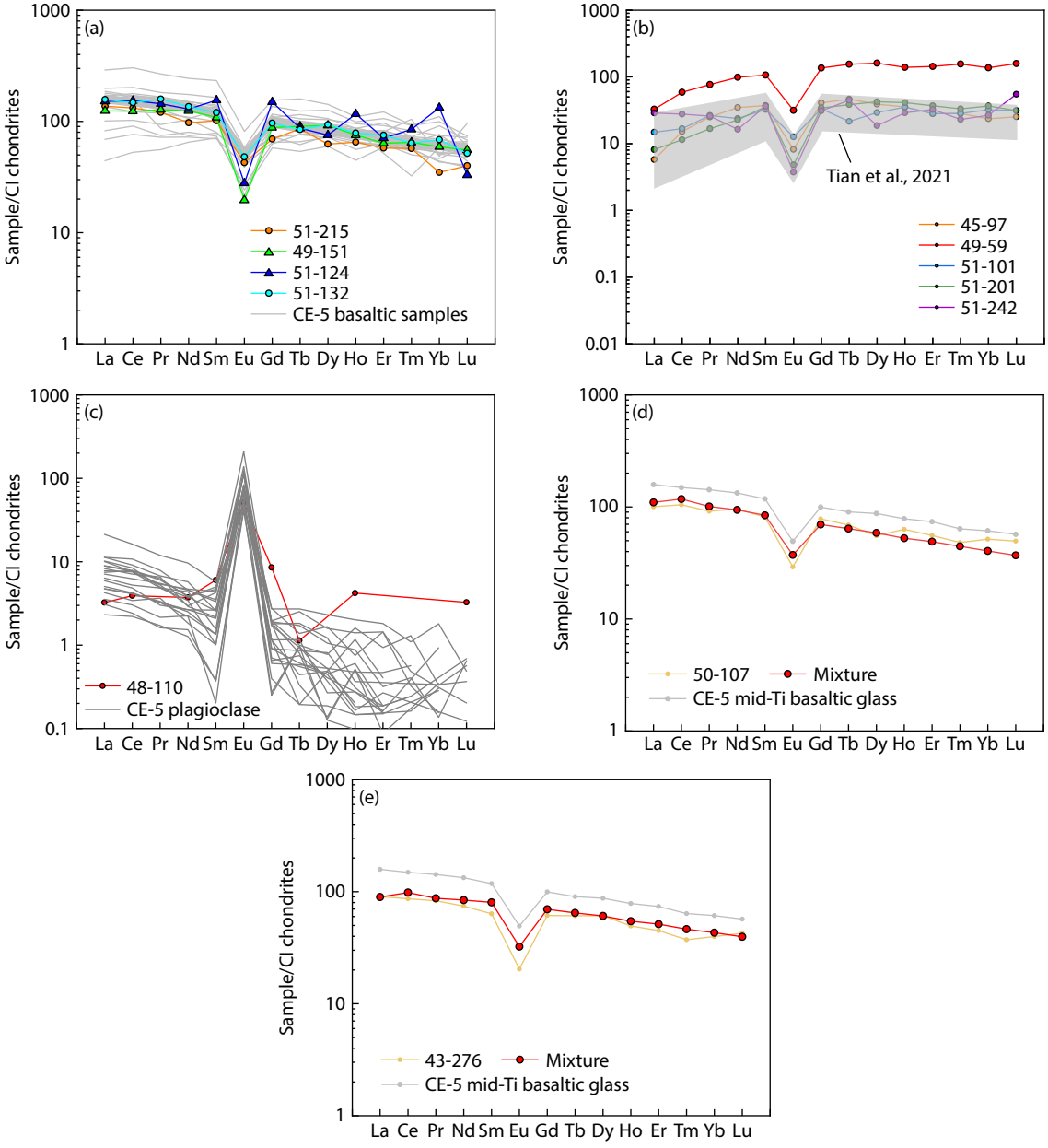

Figure 4. REE normative pattern of local glasses. (a) Basaltic glasses: these four glass patterns are almost the same as those of the CE-5 basalt (Tian HC et al., 2021; He Q et al., 2022; Li CL et al., 2022; Zong KQ et al., 2022; Jiang Y et al., 2023); (b) pyroxenitic glasses: the gray field is the CE-5 pyroxene (Tian HC et al., 2021), except 49-59; other glasses are in the gray field; (c) feldspathic glasses; (d) local mixed glass 50-107. The data on CE-5 glass is after Yang W et al. (2022). The data of CI chondrites from McDonough and Sun, 1995.

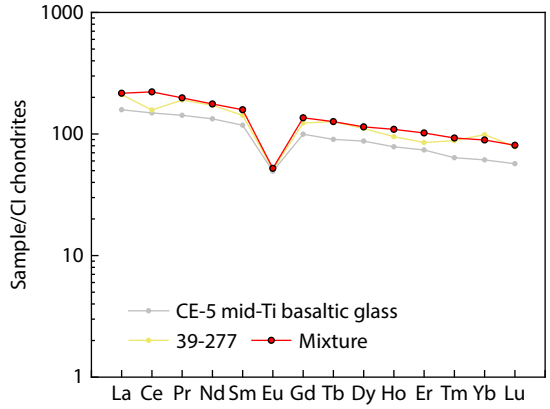

Figure 5. Exotic mixed glass (39-277) REE pattern. The red line is the mixing calculated result. The result matches the REE pattern well. We used the KREEP material 15386 to calculate the mixture. The data on 15386 are after Neal and Kramer (2003), and the CE-5 glass is after Yang W et al. (2022). The data of CI chondrites from McDonough and Sun, 1995.

of HREEs compared with the KREEP soil 15434 (Helmke et al., 1973; Figure 6c). One glass, 50-50, displays a feldspathic composition. It has high Al_2O_3 (>25 wt%) and low FeO contents (<6 wt%) with high Mg# values (>70; Table S4) and exhibit characteristics similar to those observed in the Apollo 16 samples (Figure 3), accompanied by a slightly positive Eu anomaly (Table 2 and Figure 6d). Two glasses, 44-4 and 50-14, exhibit high MgO contents (>24 wt%; Table 1) and Mg# values (>80; Table S4). Both samples have relatively low REE concentrations and exhibit an obvious Eu normative anomaly compared with the CE-5 bulk soil (Table 2). These characteristics are similar to the Mg-suite rocks (Lucey, 2006; Elardo et al., 2023; Figure 7).

Glass 51-42 exhibits a pyroxene-like composition with low Al_2O_3 (1.63 wt%) and TiO_2 contents (0.25 wt%), a high MgO content (20.28 wt%) and Mg# value (75; Table S4), and a high concentration of Cr, which seems to imply a mare provenance (Table 2). However, Bence et al. (1973) reported a high Cr concentration in highland clinopyroxene (their Cr_2O_3 content ranged from 0.36 to 0.96 wt%). In addition, the major elements and REE pattern of 51-

Table 2. Chemical composition of exotic glasses and CE-5 bulk soil.

Sample No.	CE-5 bulk soil (avg.)[a]	41-101	45-41 (avg.)	51-232	38-3 (avg.)	44-4 (avg.)	50-14 (avg.)	51-42	50-50 (avg.)	39-277	39-251
(wt%)											
SiO_2	41.5	43.7	57.8	48.2	48.4	48.0	50.2	52.9	47.7	46.1	60.2
TiO_2	5.09	8.18	2.36	1.78	0.35	1.46	1.98	0.25	0.19	3.55	0.13
Al_2O_3	11.4	14.2	13.8	18	24.0	5.32	6.75	1.63	25.1	14.7	15.1
FeO	22.7	17.6	10.5	11.0	5.01	9.96	8.3	12.2	3.58	13.0	7.43
MnO	0.28	0.17	0.12	0.14	0.08	0.3	0.38	0.22	0.09	0.16	0.11
MgO	6.3	4.09	5.9	7.53	7.63	28.1	24.4	20.3	8.75	11.2	7.35
CaO	11.5	9.64	7.09	11.4	13.7	5.96	6.97	11.7	14.2	10.5	8.21
Na_2O	0.42	0.51	0.8	0.71	0.57	0.11	0.16	0.02	0.24	0.19	1.12
K_2O	0.21	0.59	0.79	0.31	0.09	n.d.	0.04	0.01	n.d.	0.04	0.08
P_2O_5	0.26	0.76	0.05	0.44	0.04	0.03	0.03	0.05	0.04	0.03	0
(ppm)											
Li	14.8	17	43	24	11	9.33	n.d.	n.d.	9	12.6	10
B		29	n.d.[a]	30	n.d.	22.3	21.5	n.d.	1.4	18	25
Sc	62.9	26.4	22.6	23.2	12.3	31.9	34.2	48.7	5.7	38.7	3.7
V	88.9	50	27.0	53.3	35.5	114	119	286	26.8	89.7	22.1
Cr	1405	780	987	1315	1193	4603	4740	4680	1261	2040	1150
Co	32.4	28.4	7.65	33.8	4.63	2.8	0.89	39.4	0.66	14.3	2.3
Ni	18.6	76	n.d.	290	18	8	n.d.	88	0	44	9
Cu	15.3	11.8	n.d.	11.4	2.61	n.d.	2.25	n.d.	5.2	3.3	6
Zn	9.7	8	3.25	12	3.93	1.57	7.5	4	0	n.d.	n.d.
Ga	6	10.2	1.5	5.1	0.57	0.35	1.3	1.3	1.08	1.01	0.87
Rb	4.9	23	12	8.7	1.51	0.41	0.21	n.d.	0.36	0.56	1.18
Sr	351	345	172	242	122	62.2	80.7	1.8	122	249	65.9
Y	115	180	397	147.1	23.0	36.4	50.7	5.2	3.87	140	9.9
Zr	571	880	1903	402	87.0	139	182	5.7	12.5	640	41.7
Nb	36.3	56	159	43.2	7.6	9.47	11.7	0.18	0.51	43.3	4.4

Continued from Table 2

Sample No.	CE-5 bulk soil (avg.)[a]	41-101	45-41 (avg.)	51-232	38-3 (avg.)	44-4 (avg.)	50-14 (avg.)	51-42	50-50 (avg.)	39-277	39-251
Cs	0.21	0.56	0.3	0.38	0.15	0.03	0.23	0.07	0.05	0	0.03
Ba	409	770	2598	372	85	91.8	105	0.25	19.4	532	41
La	37.2	84	126	52.4	5.77	10.6	11.8	0.7	1.07	50	2.32
Ce	103	211	302	139	15.3	26.0	33.2	0.99	2.46	96.4	5.79
Pr	13.4	30.9	40.7	19.7	2.1	3.59	4.51	0.31	0.52	17.7	n.d.
Nd	61.4	139	173	87	9.23	20.0	23.7	n.d.	1.7	78.7	3.8
Sm	17.8	34.6	47.4	23.5	3.03	4.7	5.45	0.64	1.4	21.1	0.83
Eu	3	3.8	2.88	1.73	0.67	0.71	0.61	0.06	0.73	2.88	n.d.
Gd	19.8	37.9	56.7	29	3.8	6.9	8.65	1.6	0.62	24.5	0.54
Tb	3.3	6.5	11.0	4.49	0.61	1.12	1.41	0.34	0.06	4.56	n.d.
Dy	20.6	36.8	74.5	30.8	3.87	6.7	9.75	0.48	n.d.	27.3	0.36
Ho	4.1	6.9	16.4	5.94	0.89	1.38	1.91	0.12	0.09	5.19	n.d.
Er	11.2	20	47.4	16.8	2.68	4.03	5.25	0.97	n.d.	13.6	n.d.
Tm	1.5	2.58	7.13	2.43	0.34	0.56	0.71	0.23	0.06	2.18	n.d.
Yb	9.3	13.4	46.0	15.1	2.27	3.43	4.55	1.3	n.d.	15.9	0.35
Lu	1.3	1.89	6.29	1.88	0.28	0.53	0.75	n.d.	0.05	1.93	n.d.
Hf	14.5	24.4	53.7	10.2	2.3	3.58	4.9	0.37	0.06	17.3	0.26
Ta	1.8	2.67	6.92	2.13	0.35	0.48	0.69	n.d.	0.01	2.23	0.23
Pb	1.6	3.4	0.5	1.35	0.21	0.08	0.05	0.05	n.d.	0.49	0.32
Th	5.1	9.8	37	5.45	1.39	1.06	1.46	0.03	0.1	8.19	0.42
U	1.3	2.14	3.88	1.4	0.37	0.25	0.43	0	n.d.	1.19	0.03
Zr/Y	4.97	4.89	4.79	2.73	3.78	3.82	3.59	1.1	3.19	4.56	2.79
Sc/Sm	3.53	0.76	0.48	0.99	4.07	6.79	6.27	76.09	6.86	1.83	4.62
$(Eu/Eu^*)_N$	0.49	0.32	0.17	0.2	0.6	0.38	0.27	0.18	2.58	0.39	
$(Sm/Yb)_N$	2.08	2.81	1.12	1.69	1.45	1.49	1.3	0.54		1.44	2.11
$(La/Yb)_N$	2.72	4.26	1.87	2.36	1.73	2.1	1.75	0.37	1.01	2.14	1.36

[a]n.d., not detected; avg., average. The composition of CE-5 bulk soil is from Chen Y et al. (2023).

42 fall within the range of highland clinopyroxenes (Figures 2 and 8).

Two exotic glasses were identified as having mixture characteristics. Glass 39-277 has a high Mg# value (61), high Al_2O_3 (14.72 wt%) and MgO contents (11.18 wt%), and low FeO (12.95 wt%) and TiO_2 contents (3.55 wt%), with high incompatible element concentrations (e.g., REE, Th; Table 1), which can be best fitted by a mixture of 30% KREEP materials with 70% CE-5 basalt (Neal and Kramer, 2003; Figure 5 and Table S5). Glass 39-251 has high SiO_2 (60.22 wt%) and Al_2O_3 contents (15.13 wt%) and low FeO (7.35 wt%) and CaO (8.21 wt%) contents, with a high Mg# value (64; Table S4) compared with CE-5 bulk soil (Tables 2 and S4), indicative of a formation process involving the mixing of highland rocks or minerals.

4. Discussion

Although we selected 28 glasses with major elements distinct from the CE-5 bulk soil, the LA-ICP-MS analyses revealed that some of these glasses are of local origin. Therefore, it was necessary to consider the most appropriate method for correctly identifying the exotic glasses in the CE-5 soil sample.

4.1 Classification for the CE-5 Impact Glasses

Previous studies have utilized a variety of diagrams and plots to identify exotic glasses. For instance, Delano et al. (2007) presented a ternary diagram utilizing three nonvolatile lithophile elements (Ti, Mg, Al) to differentiate local and exotic glasses in Apollo 16 samples, using a line to approximate the boundary between mare and highland regions. Lucey (2006) proposed several diagrams, such as FeO versus Th and FeO versus Al_2O_3, to classify lunar samples into feldspar highland terranes (FHT), Procellarum KREEP terranes (PKT), and mare basalt, thus facilitating the identification of exotic materials. Furthermore, Korotev and Irving (2021) introduced a Sc versus Sm plot, whereas another well-known diagram is the CaO/Al_2O_3 versus MgO/Al_2O_3 plot, which uses two boundaries: one separating highland ($CaO/Al_2O_3 \leq 0.75$) from mare basalts ($CaO/Al_2O_3 \geq 0.75$), and another distinguishing mare

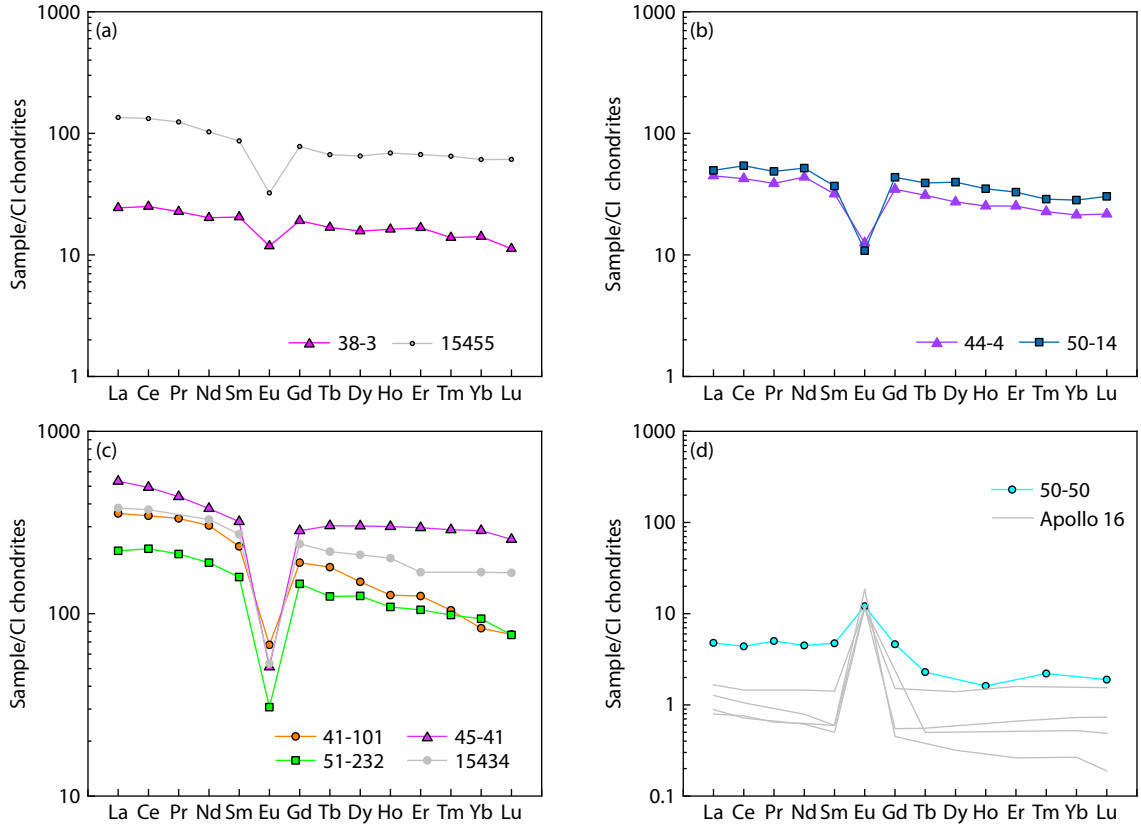

Figure 6. REE normative pattern diagram of exotic glasses. (a) REE pattern diagram of noritic glass compared with Apollo samples; (b) Mg-rich glasses; (c) REE pattern diagram of KREEP glasses compared with Apollo KREEP soil sample 15434; (d) REE pattern diagram of feldspathic glasses. The data on 15434 are from Helmke et al. (1973), and the data on 15455 are from Taylor et al. (1972). Apollo 16 samples are from Rose et al. (1973), Dymek et al. (1975), Powell et al. (1975), Wänke et al. (1975), Dominik and Jessberger (1978), Ryder and Norman (1980), Papike et al. (1997), and Norman et al. (2003). The data of CI chondrites from McDonough and Sun, 1995.

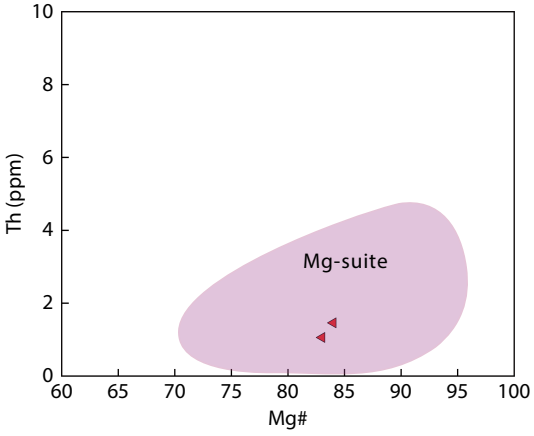

Figure 7. Mg# versus Th diagram of two Mg-rich glasses. The data cited are from Shearer et al. (2015).

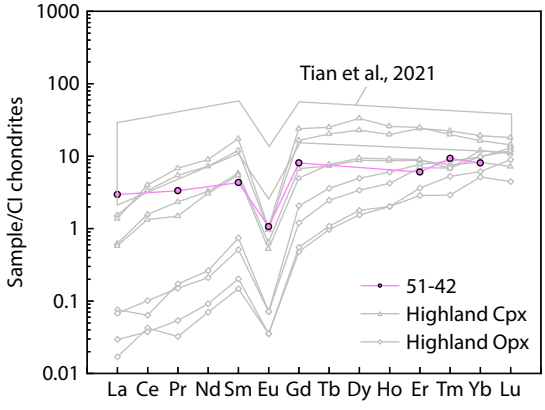

Figure 8. REE pattern diagram of highland pyroxene glass, compared with Apollo samples. Data on the CE-5 pyroxene are from Tian HC et al. (2021). Data on the highland pyroxene are from Floss et al. (1998).

basalts from picrites ($MgO/Al_2O_3 \geq 1.25$; Naney et al., 1976; Delano, 1986; Yang W et al., 2022; Wu FY et al., 2024). However, our analysis indicated that these plots were inadequate to distinguish local and exotic glasses in the CE-5 soil samples (see figures in Supplementary Material). They may misclassify some local glasses in the CE-5 soil as exotic, particularly those characterized by a single mineral composition. For example, the local feldspathic glass 48-110 appears within the highland region on those classical diagrams and plots (see figures in Supplementary Material).

To accurately identify the exotic glasses, a new classification plot (Figure 9) was implemented for the CE-5 glasses. This plot incorporates additional criteria, specifically the lanthanum (La) concentration, measured in parts per million (ppm), shown on the vertical axis, and the Mg# value, shown on the horizontal axis. These parameters were used to differentiate between locally derived

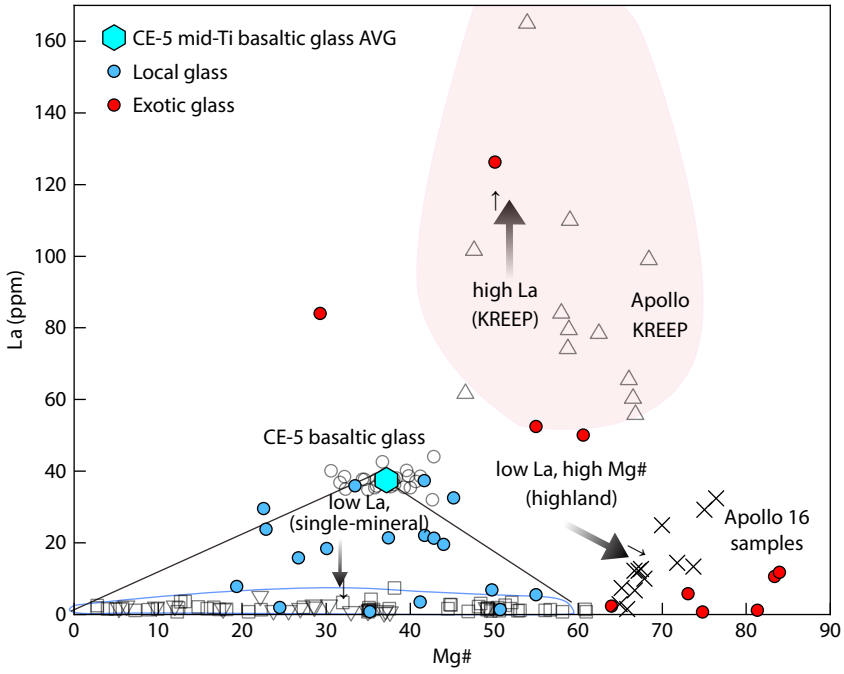

Figure 9. Plot of Mg# versus La. The triangular area represents the composition of CE-5 samples, the gray open rectangles denote CE-5 pyroxene, and the gray open inverted triangles denote the CE-5 plagioclase (mineral compositions after Tian HC et al., 2021). The gray open dots denote the CE-5 mid-Ti basaltic glass (after Yang W et al., 2022). The results falling into the triangular area represent local glasses; otherwise, they represent exotic glasses. The area circled by a blue line represents single mineral components in CE-5 samples, and the area between the blue line and the CE-5 basaltic glass area represents the local mixture materials. The black x's are Apollo 16 samples, and the data are after Taylor et al. (1973, 1974), Wänke et al. (1973), Morris et al. (1986), Korotev (1997), and Norman et al. (2010). The small gray triangles are noted as Apollo KREEP samples, and the data are after Hubbard et al. (1973), Wänke et al. (1976, 1977), Warren and Wasson (1980), Lindstrom (1984), Salpas et al. (1987), Ryder and Sherman (1989), Simon et al. (1989), and Neal and Kramer (2003). AVG, average.

and exotic glasses. We referred to Mg# values (Mg# < 60) and the La concentration of the CE-5 basaltic samples (Che XC et al., 2021; Hu S et al., 2021; Tian HC et al., 2021; He Q et al., 2022; Wu FY et al., 2024) to determine whether the glasses were within these end member boundaries (see Figure 9).

On the one hand, the Mg# value represents a major difference between the CE-5 mare basalts and the highland rocks. The Mg# values in the minerals of the CE-5 basalt are lower than 60 (Che XC et al., 2021; Hu S et al., 2021; Tian HC et al., 2021; He Q et al., 2022; Chen Y et al., 2023; Wu FY et al., 2024). In contrast, the highland minerals have higher Mg# (>65; Taylor et al., 1973, 1974; Wänke et al., 1973; Morris et al., 1986; Korotev, 1997; Norman et al., 2010). On the other hand, most CE-5 basalt fragments have La concentrations ranging from 30 to 45 ppm (Li CL et al., 2021; Tian HC et al., 2021; He Q et al., 2022; Zong KQ et al., 2022; Jiang Y et al., 2023). The minerals in the CE-5 basalt have lower La concentrations, which are usually less than 8 ppm (Tian HC et al., 2021). In contrast, KREEP samples exhibit La concentrations higher than 50 ppm (Hubbard et al., 1973; Wänke et al., 1976, 1977; Warren and Wasson, 1980; Lindstrom, 1984; Salpas et al., 1987; Ryder and Sherman, 1989; Simon et al., 1989; Neal and Kramer, 2003). Despite the fact that the highland samples have a wide range of La concentrations, from several to 40 ppm (Taylor et al., 1973, 1974; Wänke et al., 1973; Morris et al., 1986; Korotev, 1997; Norman et al., 2010; Figure 9), they can be distinguished from the CE-5 local materials through combined analysis of La with Mg#. A comparison of the traditional classification plots or diagrams revealed that the Mg# versus La plot provides a more definitive classification of glasses, particularly those composed predominantly of a single mineral phase (Figure 9). The application of this plot to glasses in other lunar soil samples has yet to be determined and will require further investigation in the future.

Despite the major element compositions of exotic glasses compared with the CE-5 basaltic component of the local glasses identified in this study, trace element analysis indicated that their material was still sourced from the local unit. Wu YH et al. (2023) identified a glass (G133) with distinct chemical characteristics compared with CE-5 local regolith. They proposed that the observed chemical variations could result from the selective melting of a relatively uniform protolith during local impacts. Our study identified more such glasses, providing additional support for their study. It should be noted that all these glasses are small in diameter (<70 μm; Wang BW et al., 2024; Figure S1 and Table S4), and the G133 is merely 45 μm (Wu YH et al., 2023). The small sizes of these glasses also support the view that these glasses were formed by a selective impact melting process of local materials. Furthermore, Chao et al. (1970) suggested that larger glass particles more accurately reflect the bulk composition of the original targets, given the challenges in determining the fraction or bulk composition of smaller discrete glasses. The formation of these local glasses suggests the need to extend our consideration of selective melting processes (not only mare basalts or bulk soil

components) to encompass both single mineral and mixtures in major and trace elements. This expanded approach provides a more robust framework for interpreting the classification and provenance characteristics of CE-5 impact glasses, particularly in terms of reconciling their chemical signatures with potential precursor materials. Therefore, to determine the provenance of smaller impact glasses, it is essential to analyze not only the major elements, but also the trace elements.

In the case of the local pyroxene-like glasses, subsurface cumulate has been suggested as another possible origin (Su B et al., 2022; Zong KQ et al., 2022; Wu FY et al., 2024). However, these glasses exhibit low Mg# values (<52), which may be inconsistent with the potential high Mg# of the subsurface cumulate layer. On the basis of the Mg-Fe partition coefficient (Putirka, 2008), the CE-5 basalt with Mg# values of ~30 should equilibrate with pyroxenes with Mg# values of ~60. This indicates that the Mg# of subsurface cumulate should be ≥60. In addition, these pyroxene-like glasses all have small diameters (<70 μm), which also supports the view that they were derived from selective melting of local materials.

4.2 Potential Provenance of the Exotic Glasses

Impact cratering is the fundamental mechanism for the transportation of materials on the lunar surface (Delano, 1991; Korotev and Gillis, 2001; Zellner et al., 2002; Zeigler et al., 2006; Yan P et al., 2022; Yang W et al., 2022). Although the provenance of the exotic glasses is highly speculative, these glasses can provide the chemical composition and further understanding of materials not sampled on the lunar surface. For example, they can serve to corroborate previous studies (e.g., Zeigler et al., 2006) or provide direction for future ejecta simulation studies in lunar exploration (e.g., Černok et al., 2021). Ten glasses exhibited exotic chemical compositions, and remote sensing data provide a means of determining their potential provenance. Previous remote sensing data have suggested that the Aristarchus, Pythagoras, Mairan, Sharp, Harpalus, and Copernicus craters could potentially serve as sources of exotic materials for the CE-5 landing site (Xie MG et al., 2020; Fu XH et al., 2021; Qian YQ et al., 2021).

The analysis of remote sensing data from the M^3 (Moon, Mineral, Mapper) instrument, and Kaguya has revealed the presence of noritic composition, high-Ca pyroxene, a high Mg# zone, and feldspar materials in the Aristarchus crater (McEwen et al.,1994; Mustard et al., 2011; Zhang L et al., 2023), as well as being a potential source of KREEP material with a high Th concentration (Th ≥ 8 ppm; Lawrence et al., 2007; Fu XH et al., 2021) and a high FeO content (>16 wt%; Fu XH et al., 2021). Other craters, such as the Mairan (Th ≥ 11 ppm) and Sharp (Th ≥ 8 ppm), were also noted as potential sources of KREEP materials but with lower FeO contents (≤15 wt%; Fu XH et al., 2021). Otherwise, the Pythagoras crater was considered a potential source of feldspathic materials (Fu XH et al., 2021). Moreover, Mei AX et al. (2023) identified a mare–highland mixture breccia (CE5C) containing KREEP materials and proposed that it may originate from the eastern region of the CE-5 landing site, given the location of the Mairan crater to the east of the CE-5 landing site. According to the chemical results for exotic glasses and remote sensing data, we assume the potential provenance will provide the possibility for future research (Table 3).

5. Conclusions

The impact glasses present in the CE-5 soil samples offer valuable insights into the diversity of the lunar surface. The findings of our study can be summarized as follows:

(1) Although all 28 glasses studied here exhibit major element compositions distinct from those of the CE-5 bulk soil, 18 of them have chemical compositions similar to those of the CE-5 basaltic samples or minerals in the basalt, indicating a local origin. Therefore, a more comprehensive investigation is necessary to accurately identify the exotic materials, particularly for glasses characterized by a single mineral composition and small-diameter glasses. We propose a novel classification plot, Mg# versus La, to more effectively identify the exotic glasses in the CE-5 samples, thereby providing constraints for a better understanding of the characteristics of exotic materials in these samples.

Table 3. The possible provenance of exotic glasses.

No.	Main characteristics	Possible provenance	Distance[a] (km)
38-3	Has noritic content. REE pattern characteristics similar to those of Apollo samples, with a high value of plagioclase.	Aristarchus crater wall	600
39-251	High plagioclase and low Ca pyroxene contents, higher Mg# than CE-5 samples; may involve the mixing of highland rocks or minerals.	Aristarchus crater	600
39-277	High Mg# (61) and La (50 ppm), more than in CE-5 samples. Mixed with KREEP materials.	The KREEP materials may be from the Mairan crater	200
44-4, 50-14	High MgO and Mg# values, low REEs, and an obvious Eu-negative anomaly.	Aristarchus crater	600
41-101, 45-41, 51-232	KREEP. High concentration of REEs, similar to and even higher than KREEP basalt 15386; 41-101 exhibits a high value of FeO, but 45-41 and 51-232 display low FeO.	45-4, 51-232: Mairan or Sharp crater; 41-101: Aristarchus crater	Mairan: 200 Aristarchus: 600 Sharp: 265.5
50-50	Feldspathic. High composition of Al_2O_3, a slight Eu-positive anomaly, and higher Mg# than in CE-5 samples.	Pythagoras or Aristarchus crater	Pythagoras: 650 Aristarchus: 600
51-42	Characteristics similar to highland clinopyroxene in both major and trace elements; higher Mg# than in CE-5 samples.	Aristarchus crater	600

[a]The distance measurement used in QuickMap (https://quickmap.lroc.asu.edu/).

(2) The remaining 10 glasses are identified as exotic and exhibit a range of chemical characteristics. We suggest, based on remote sensing data, that these exotic glasses may have originated from the Aristarchus, Mairan, Sharp, and Pythagoras craters.

Acknowledgments

The Chang'e-5 lunar samples were provided by the China National Space Administration. This study was funded by the National Natural Science Foundation of China (Grant Nos. 42241103 and 62227901) and the Key Research Program of the Institute of Geology and Geophysics, Chinese Academy of Sciences (Grant Nos. IGGCAS-202101 and IGGCAS-202401). We thank the two anonymous reviewers for their valuable suggestions.

Supplementary Material

Supplementary tables and figures to this article can be found in the Supplementary Material.

References

Bence, A., Papike, J., Sueno, S., and Delano, J. (1973). Pyroxene poikiloblastic rocks from the lunar highlands. *Paper presented at the Proceedings of the Lunar Science Conference*, *4*, 597.

Černok, A., White, L. F., Anand, M., Tait, K. T., Darling, J. R., Whitehouse, M., ... Ghent, R. (2021). Lunar samples record an impact 4.2 billion years ago that may have formed the Serenitatis Basin. *Communications Earth & Environment*, *2*(1), 120. https://doi.org/10.1038/s43247-021-00181-z

Chao, E. C. T., Boreman, J. A., Minkin, J. A., James, O. B., and Desborough, G. A. (1970). Lunar glasses of impact origin: Physical and chemical characteristics and geologic implications. *J. Geophys. Res.*, *75*(35), 7445–7479. https://doi.org/10.1029/JB075i035p07445

Che, X. C., Nemchin, A., Liu, D. Y., Long, T., Wang, C., Norman, M. D., Joy, K. H., Tartese, R., Head, J., … Webb, S. G. (2021). Age and composition of young basalts on the Moon, measured from samples returned by Chang'e-5. *Science, 374*(6569), 887–890. https://doi.org/10.1126/science.abl7957

Chen, Y., Hu, S., Li, J. H., Li, Q. L., Li, X. Y., Li, Y., Liu, Y., Qian, Y. Q., Yang, W., ... Li, X. H. (2023). Chang'e-5 lunar samples shed new light on the Moon. *Innov. Geosci.*, *1*(1), 100014. https://doi.org/10.59717/j.xinn-geo.2023.100014

Delano, J. W., Lindsley, D. H., and Rudowski, R. (1982). Glasses of impact origin from Apollo 11, 12, 15, and 16-Evidence for fractional vaporization and mare/highland mixing. *In Lunar and Planetary Science Conference*, 12th, Houston, TX, March 16-20, 1981, Proceedings. Section 1. (A82-31677 15-91), (Vol. 12, pp. 339–370). New York and Oxford: Pergamon Press

Delano, J. W. (1986). Pristine lunar glasses: Criteria, data, and implications. *J. Geophys. Res.: Solid Earth*, *91*(B4), 201–213. https://doi.org/10.1029/JB091iB04p0D201

Delano, J. W. (1991). Geochemical comparison of impact glasses from lunar meteorites ALHA81005 and MAC88105 and Apollo 16 regolith 64001. *Geochim. Cosmochim. Acta*, *55*(11), 3019–3029. https://doi.org/10.1016/0016-7037(91)90470-P

Delano, J. W., Zellner, N. E. B., Barra, F., Olson, E., Swindle, T. D., Tibbetts, N. J., and Whittet, D. C. B. (2007). An integrated approach to understanding Apollo 16 impact glasses: Chemistry, isotopes, and shape. *Meteorit. Planet. Sci.*, *42*(6), 993–1004. https://doi.org/10.1111/j.1945-5100.2007.tb01146.x

Dominik, B., and Jessberger, E. K. (1978). Early lunar differentiation: 4.42-AE-old plagioclase clasts in Apollo 16 breccia 67435. *Earth Planet. Sci. Lett.*, *38*(2), 407–415. https://doi.org/10.1016/0012-821X(78)90115-2

Dymek, R. F., Albee, A. L., and Chodos, A. A. (1975). Comparative petrology of lunar cumulate rocks of possible primary origin: Dunite 72415, troctolite 76535, norite 78235, and anorthosite 62237. In *Proceedings of the 6th Lunar Science Conference* (pp. 301–341). New York: Pergamon Press, Inc.

Elardo, S. M., Pieters, C. M., Dhingra, D., Hanna, K. L. D., Glotch, T. D., Greenhagen, B. T., Gross, J., Head, J. W., Jolliff, B. L., … Ohtake, M. (2023). The evolution of the lunar crust. *Rev. Mineral. Geochem.*, *89*(1), 293–338. https://doi.org/10.2138/rmg.2023.89.07

Floss, C., James, O. B., McGee, J. J., and Crozaz, G. (1998). Lunar ferroan anorthosite petrogenesis: Clues from trace element distributions in FAN subgroups. *Geochim. Cosmochim. Acta*, *62*(7), 1255–1283. https://doi.org/10.1016/S0016-7037(98)00031-3

Fu, X. H., Hou, X. T., Zhang, J., Li, B., Ling, Z. C., Jolliff, B. L., Xu, L., and Zou, Y. L. (2021). Possible non-mare lithologies in the regolith at the Chang'E-5 landing site: Evidence from remote sensing data. *J. Geophys. Res.: Planets*, *126*(5), e2020JE006797. https://doi.org/10.1029/2020je006797

Hao, J. L., Yang, W., He, H. C., Zhang, D., Hu, S., Tian, H. C., Li, R. Y., and Lin, Y. T. (2024). Submicron spatial resolution Pb-Pb dating for the formation age of Chang'e-5 basalt. *Lithos*, *468–469*, 107495. https://doi.org/10.1016/j.lithos.2024.107495

He, Q., Li, Y. H., Baziotis, I., Qian, Y. Q., Xiao, L., Wang, Z. C., Zhang, W., Luo, B. J., Neal, C. R., … Wang, L. (2022). Detailed petrogenesis of the unsampled Oceanus Procellarum: The case of the Chang'e-5 mare basalts. *Icarus*, *383*, 115082. https://doi.org/10.1016/j.icarus.2022.115082

Helmke, P. A., Blanchard, D. P., Haskin, L. A., Telander, K., Weiss, C., and Jacobs, J. W. (1973). Major and trace elements in igneous rocks from Apollo 15. *Moon, 8*(1), 129–148. https://doi.org/10.1007/BF00562754

Hu, S., He, H. C., Ji, J. L., Lin, Y. T., Hui, H. J., Anand, M., Tartèse, R., Yan, Y. H., Hao, J. L., … Ouyang, Z. Y. (2021). A dry lunar mantle reservoir for young mare basalts of Chang'e-5. *Nature, 600*(7887), 49–53. https://doi.org/10.1038/s41586-021-04107-9

Hubbard, N. J., Rhodes, J. M., Gast, P. W., Bansal, B. M., Shih, C. Y., Wiesmann, H. E. N. R. Y., and Nyquist, L. E. (1973). Lunar rock types: The role of plagioclase in non-mare and highland rock types. In *Proceedings of the Lunar Science Conference*, (Vol. 4, p. 1297).

Jiang, Y., Li, Y., Liao, S. Y., Yin, Z. J., and Hsu, W. (2022). Mineral chemistry and 3D tomography of a Chang'E 5 high-Ti basalt: Implication for the lunar thermal evolution history. *Sci. Bull.*, *67*(7), 755–761. https://doi.org/10.1016/j.scib.2021.12.006

Jiang, Y., Kang, J. T., Liao, S. Y., Elardo, S. M., Zong, K. Q., Wang, S. J., Nie, C., Li, P. Y., Yin, Z. J., … Hsu, W. (2023). Fe and Mg isotope compositions indicate a hybrid mantle source for young Chang'E 5 mare basalts. *Astrophys. J. Lett.*, *945*(2), L26. https://doi.org/10.3847/2041-8213/acbd31

Jochum, K. P., Willbold, M., Raczek, I., Stoll, B., and Herwig, K. (2005). Chemical characterisation of the USGS reference glasses GSA-1G, GSC-1G, GSD-1G, GSE-1G, BCR-2G, BHVO-2G and BIR-1G using EPMA, ID-TIMS, ID-ICP-MS and LA-ICP-MS. *Geostand. Geoanal. Res.*, *29*(3), 285–302. https://doi.org/10.1111/j.1751-908X.2005.tb00901.x

Jochum, K. P., Weis, U., Stoll, B., Kuzmin, D., Yang, Q. C., Raczek, I., Jacob, D. E., Stracke, A., Birbaum, K., … Enzweiler, J. (2011). Determination of reference values for NIST SRM 610–617 glasses following ISO guidelines. *Geostand. Geoanal. Res.*, *35*(4), 397–429. https://doi.org/10.1111/j.1751-908X.2011.00120.x

Korotev, R. L., Haskin, L. A., and Jolliff, B. L. (1995). A simulated geochemical rover mission to the Taurus-Littrow valley of the Moon. *J. Geophys. Res.: Planets*, *100*(E7), 14403–14420. https://doi.org/10.1029/95JE01670

Korotev, R. L. (1997). Some things we can infer about the Moon from the composition of the Apollo 16 regolith. *Meteorit. Planet. Sci.*, *32*(4), 447–478. https://doi.org/10.1111/j.1945-5100.1997.tb01291.x

Korotev, R. L., and Gillis, J. J. (2001). A new look at the Apollo 11 regolith and KREEP. *J. Geophys. Res.: Planets*, *106*(E6), 12339–12353. https://doi.org/10.1029/2000je001336

Korotev, R. L., Zeigler, R. A., and Floss, C. (2010). On the origin of impact glass in the Apollo 16 regolith. *Geochim. Cosmochim. Acta*, *74*(24), 7362–7388. https://doi.org/10.1016/j.gca.2010.09.020

Korotev, R. L., and Irving, A. J. (2021). Lunar meteorites from northern Africa. *Meteorit. Planet. Sci.*, *56*(2), 206–240. https://doi.org/10.1111/maps.13617

Lawrence, D. J., Puetter, R. C., Elphic, R. C., Feldman, W. C., Hagerty, J. J., Prettyman, T. H., and Spudis, P. D. (2007). Global spatial deconvolution of Lunar Prospector Th abundances. *Geophys. Res. Lett.*, *34*(3), L03201. https://doi.org/10.1029/2006gl028530

Li, C. L., Hu, H., Yang, M. F., Pei, Z. Y., Zhou, Q., Ren, X., Liu, B., Liu, D. W., Zeng, X. G., ... Ouyang, Z. Y. (2022). Characteristics of the lunar samples returned by the Chang'E-5 mission. *Natl. Sci. Rev.*, *9*(2), nwab188. https://doi.org/10.1093/nsr/nwab188

Li, Q. L., Zhou, Q., Liu, Y., Xiao, Z. Y., Lin, Y. T., Li, J. H., Ma, H. X., Tang, G. Q., Guo, S., ... Li, X. H. (2021). Two-billion-year-old volcanism on the Moon from Chang'e-5 basalts. *Nature*, *600*(7887), 54–58. https://doi.org/10.1038/s41586-021-04100-2

Lindstrom, M. M. (1984). Alkali gabbronorite, ultra-KREEPy melt rock and the diverse suite of clasts in North Ray Crater feldspathic fragmental breccia 67975. *J. Geophys. Res.: Solid Earth*, *89*(S01), C50–C62. https://doi.org/10.1029/JB089iS01p00C50

Long, T., Qian, Y., Norman, M. D., Miljkovic, K., Crow, C., Head, J. W., ... Nemchin, A. (2022). Constraining the formation and transport of lunar impact glasses using the ages and chemical compositions of Chang'e-5 glass beads. *Science Advances*, *8*(39). https://doi.org/10.1126/sciadv.abq2542

Lucey, P. (2006). Understanding the lunar surface and space-moon interactions. *Rev. Mineral. Geochem.*, *60*(1), 83–219. https://doi.org/10.2138/rmg.2006.60.2

Maxwell, J. A., and Wiik, H. B. (1971). Chemical composition of Apollo 12 lunar samples 12004, 12033, 12051, 12052 and 12065. *Earth Planet. Sci. Lett. Earth Planet. Sci. Lett.*, *10*(3), 285–288. https://doi.org/10.1016/0012-821X(71)90032-X

McDonough, W. F., and Sun, S. S. (1995). The composition of the Earth. *Chem. Geol.*, *120*(3-4), 223–253. https://doi.org/10.1016/0009-2541(94)00140-4

McEwen, A. S., Robinson, M. S., Eliason, E. M., Lucey, P. G., Duxbury, T. C., and Spudis, P. D. (1994). Clementine observations of the Aristarchus region of the Moon. *Science*, *266*(5192), 1858–1862. https://doi.org/10.1126/science.266.5192.1858

Mei, A. X., Jiang, Y., Liao, S. Y., Kang, J. T., Huang, F., and Hsu, W. (2023). KREEP-rich breccia in Chang'E-5 regolith and its implications. *Sci. China Earth Sci.*, *66*(11), 2473–2486. https://doi.org/10.1007/s11430-022-1134-0

Meyer Jr, C. (1978). Ion microprobe analyses of aluminous lunar glasses-A test of the 'rock type' hypothesis. In *Lunar and Planetary Science Conference, 9th*, Houston, Tex., March 13–17, 1978, Proceedings. Volume 2 (A79-39176 16-91). (Vol. 9, p. 1551–1570). New York: Pergamon Press, Inc.

Morris, R. V., See, T. H., and Hörz, F. (1986). Composition of the Cayley formation at Apollo 16 as inferred from impact melt splashes. *J. Geophys. Res.: Solid Earth*, *91*(B13), E21–E42. https://doi.org/10.1029/JB091iB13p00E21

Mustard, J. F., Pieters, C. M., Isaacson, P. J., Head, J. W., Besse, S., Clark, R. N., Klima, R. L., Petro, N. E., Staid, M. I., … Tompkins, S. (2011). Compositional diversity and geologic insights of the Aristarchus crater from Moon Mineralogy Mapper data. *J. Geophys. Res.*, *116*, E00G12. https://doi.org/10.1029/2010je003726

Naney, M., Crowl, D., and Papike, J. (1976). The Apollo 16 drill core: Statistical analysis of glass chemistry and the characterization of a high alumina-silica poor (HASP) glass. In *Proceedings of the 7th Lunar Science Conference* (pp. 155–184). New York: Pergamon Press, Inc.

Neal, C. R., and Kramer, G. Y. (2003). The composition of KREEP: a detailed study of KREEP basalt 15386. In *Lunar and Planetary Science XXXIV, Houston*. New York: Pergamon Press.

Norman, M. D., Borg, L. E., Nyquist, L. E., and Bogard, D. D. (2003). Chronology, geochemistry, and petrology of a ferroan noritic anorthosite clast from Descartes breccia 67215: Clues to the age, origin, structure, and impact history of the lunar crust. *Meteorit. Planet. Sci.*, *38*(4), 645–661. https://doi.org/10.1111/j.1945-5100.2003.tb00031.x

Norman, M. D., Duncan, R. A., and Huard, J. J. (2010). Imbrium provenance for the Apollo 16 Descartes terrain: Argon ages and geochemistry of lunar breccias 67016 and 67455. *Geochim. Cosmochim. Acta*, *74*(2), 763–783. https://doi.org/10.1016/j.gca.2009.10.024

Norman, M. D., Jourdan, F., and Hui, S. S. M. (2019). Impact history and regolith evolution on the moon: Geochemistry and ages of glasses from the Apollo 16 site. *J. Geophys. Res.: Planets*, *124*(12), 3167–3180. https://doi.org/10.1029/2019je006053

Papike, J. J., Fowler, G. W., and Shearer, C. K. (1997). Evolution of the lunar crust: SIMS study of plagioclase from ferroan anorthosites. *Geochim. Cosmochim. Acta*, *61*(11), 2343–2350. https://doi.org/10.1016/S0016-7037(97)00086-0

Powell, B. N., Dungan, M. A., and Weiblen, P. W. (1975). Apollo 16 feldspathic melt rocks: Clues to the magmatic history of the lunar crust. In *Proceedings of the 6th Lunar Science Conference* (pp. 415–433). New York: Pergamon Press, Inc.

Putirka, K. D. (2008). Thermometers and barometers for volcanic systems. *Rev. Mineral. Geochem.*, *69*(1), 61–120. https://doi.org/10.2138/rmg.2008.69.3

Qian, Y. Q., Xiao, L., Wang, Q., Head, J. W., Yang, R. H., Kang, Y., van der Bogert, C. H., Hiesinger, H., Lai, X. M., … Zhao, S. Y. (2021). China's Chang'e-5 landing site: Geology, stratigraphy, and provenance of materials. *Earth Planet. Sci. Lett.*, *561*, 116855. https://doi.org/10.1016/j.epsl.2021.116855

Rhodes, J., Blanchard, D., Dungan, M., Brannon, J., and Rodgers, K. (1977). Chemistry of Apollo 12 mare basalts-Magma types and fractionation processes. In *Lunar Science Conference, 8th*, Houston, Tex., March 14-18, 1977, Proceedings. Volume 2 (A78-41551 18-91). New York: Pergamon Press, Inc., p.1305–1338.

Rose Jr, H. J., Cuttitta, F., Berman, S., Carron, M. K., Christian, R. P., Dwornik, E. J., ... Ligon Jr, D. T. (1973). Compositional data for twenty-two Apollo 16 samples. In *Proceedings of the Lunar Science Conference*, Vol. 4, p. 1149.

Ryder, G., and Norman, M. D. (1980). *Catalog of Apollo 16 Rocks: Part 3. 67015–69965*. Houston, Texas: Lyndon B. Johnson Space Center.

Ryder, G., and Sherman, S. B. (1989). *The Apollo 15 Coarse Fines (4–10 mm)*. Houston, Texas: Lyndon B. Johnson Space Center.

Salpas, P. A., Taylor, L. A., and Lindstrom, M. M. (1987). Apollo 17 KREEPy basalts: Evidence for nonuniformity of KREEP. *J. Geophys. Res.: Solid Earth*, *92*(B4), E340–E348. https://doi.org/10.1029/JB092iB04p0E340

Shearer, C. K., Elardo, S. M., Petro, N. E., Borg, L. E., and McCubbin, F. M. (2015). Origin of the lunar highlands Mg-suite: An integrated petrology, geochemistry, chronology, and remote sensing perspective. *Am. Mineral.*, *100*(1), 294–325. https://doi.org/10.2138/am-2015-4817

Simon, S. B., Papike, J. J., Shearer, C. K., Hughes, S. S., and Schmitt, R. A. (1989). Petrology of Apollo 14 regolith breccias and ion microprobe studies of glass beads. In *Proceedings of the 19th Lunar and Planetary Science Conference* (pp. 1–17). Houston, Texas: Lunar and Planetary Institute.

Snyder, G. A., Neal, C. R., Taylor, L. A., and Halliday, A. N. (1997). Anatexis of lunar cumulate mantle in time and space: Clues from trace-element, strontium, and neodymium isotopic chemistry of parental Apollo 12 basalts. *Geochim. Cosmochim. Acta*, *61*(13), 2731–2747. https://doi.org/10.1016/S0016-7037(97)00082-3

Su, B., Yuan, J. Y., Chen, Y., Yang, W., Mitchell, R. N., Hui, H. J., Wang, H., Tian, H. C., Li, X. H., and Wu, F. Y. (2022). Fusible mantle cumulates trigger young mare volcanism on the cooling Moon. *Sci. Adv.*, *8*(42), eabn2103. https://doi.org/10.1126/sciadv.abn2103

Taylor, S.R., Gorton, M.P., Muir, P., Nance W., Rudowski R., and Ware, N. (1972). Composition of the lunar highlands, II. The apenine front. In *The Apollo 15 Lunar Samples*. Houston, Texas: The Lunar Science Institute, 262–264 (abstract).

Taylor, S. R., Gorton, M. P., Muir, P., Nance, W. B., Rudowski, R., and Ware, N. (1973). Composition of the Descartes region, lunar highlands. *Geochim. Cosmochim. Acta*, *37*(12), 2665–2683. https://doi.org/10.1016/0016-7037(73)90271-8

Taylor, S. R., Gorton, M., Muir, P., Nance, W., Rudowski, R., and Ware, N. (1974). Lunar highland composition. *Abstr. Lunar Planet. Sci. Conf.*, *5*, 789.

Tian, H. C., Wang, H., Chen, Y., Yang, W., Zhou, Q., Zhang, C., Lin, H. L., Huang, C., Wu, S. T., … Wu, F. Y. (2021). Non-KREEP origin for Chang'e-5 basalts in the Procellarum KREEP Terrane. *Nature*, *600*(7887), 59–63. https://doi.org/10.1038/s41586-021-04119-5

Wakita, H., Rey, P., and Schmitt, R. A. (1971). Abundances of the 14 rare-Earth elements and 12 other trace elements in Apollo 12 samples: Five igneous and one breccia rocks and four soils. In *Proceedings of the 2nd Lunar Science Conference* (pp. 1319–1329). Oxford, UK: Pergamon Press.

Wang, B. W., Zhang, Q. W. L., Chen, Y., Zhao, W. H., Liu, Y., Tang, G. Q., Ma, H. X., Su, B., Hui, H. J., … Li, Q. L. (2024). Returned samples indicate volcanism on the Moon 120 million years ago. *Science*, *385*(6713), 1077–1080. https://doi.org/10.1126/science.adk6635

Wänke, H., Baddenhausen, H., Dreibus, G., Jagoutz, E., Kruse, H., Palme, H., ...

Teschke, F. (1973). Multielement analyses of Apollo 15, 16, and 17 samples and the bulk composition of the moon. In *Proceedings of the Lunar Science Conference*, Vol. 4, p. 1461.

Wänke, H., Palme, H., Baddenhausen, H., Dreibus, G., Jagoutz, E., Kruse, H., and Thacker, R. (1975). New data on the chemistry of lunar samples: Primary matter in the lunar highlands and the bulk composition of the moon. In *Proceedings of the 6th Lunar Science Conference* (pp. 1313–1340). New York: Pergamon Press, Inc.

Wänke, H., Palme, H., Kruse, H., Baddenhausen, H., Cendales, M., Dreibus, G., Hofmeister, H., Jagoutz, E., Palme, C., … Thacker, R. (1976). Chemistry of lunar highland rocks: A refined evaluation of the composition of the primary matter. In *Proceedings of the 7th Lunar Science Conference* (pp. 3479–3499). New York: Pergamon Press, Inc.

Wänke, H., Baddenhausen, H., Blum, K., Cendales, M., Dreibus, G., Hofmeister, H., Kruse, H., Jagoutz, E., Palme, C., … Vilcsek, E. (1977). On the chemistry of lunar samples and achondrites. Primary matter in the lunar highlands: A re-evaluation. In *Proceedings of the 8th Lunar Science Conference* (pp. 2191–2213). New York: Pergamon Press, Inc.

Warren, P. H., and Wasson, J. T. (1980). Further foraging for pristine nonmare rocks: Correlations between geochemistry and longitude. In *Proceedings of the 11th Lunar and Planetary Science Conference* (pp. 431–4700). New York: Pergamon Press, Inc.

Wu, F. Y., Li, Q. L., Chen, Y., Hu, S., Yue, Z. Y., Zhou, Q., Wang, H., Yang, W., Tian, H. C., … Delano, J. W. (2024). Lunar evolution in light of the Chang'e-5 returned samples. *Annu. Rev. Earth Planet. Sci.*, *52*, 159–194. https://doi.org/10.1146/annurev-earth-040722-100453

Wu, S. T., Huang, C., Xie, L. W., Yang, Y. H., and Yang, J. H. (2018). Iolite based bulk normalization as 100% (*m/m*) quantification strategy for reduction of laser ablation-inductively coupled plasma-mass spectrometry transient signal. *Chin. J. Anal. Chem.*, *46*(10), 1628–1636. https://doi.org/10.1016/s1872-2040(18)61118-1

Wu, S. T., Wörner, G., Jochum, K. P., Stoll, B., Simon, K., and Kronz, A. (2019). The preparation and preliminary characterisation of three synthetic andesite reference glass materials (ARM-1, ARM-2, ARM-3) for *in situ* microanalysis. *Geostand. Geoanal. Res.*, *43*(4), 567–584. https://doi.org/10.1111/ggr.12301

Wu, Y. H., Liao, S. Y., Yan, P., Xiao, Z. Y., Yin, Z. J., Yang, W., Wang, H., Tian, H. C., Hui, H. J., … Hsu, W. (2023). Impact-related chemical modifications of the Chang'E-5 lunar regolith. *Geochim. Cosmochim. Acta*, *363*, 94–113. https://doi.org/10.1016/j.gca.2023.10.031

Xie, M. G., Xiao, Z. Y., Zhang, X. Y., and Xu, A. A. (2020). The provenance of regolith at the Chang'e-5 candidate landing region. *J. Geophys. Res.: Planets, 125*(5). https://doi.org/10.1029/2019je006112

Yan, P., Xiao, Z. Y., Wu, Y. H., Yang, W., Li, J. H., Gu, L. X., Liao, S. Y., Yin, Z. J., Wang, H., ... Li, X. H. (2022). Intricate regolith reworking processes revealed by microstructures on lunar impact glasses. *J. Geophys. Res.: Planets*, *127*(12), e2022JE007260. https://doi.org/10.1029/2022je007260

Yan, P., Xiao, Z. Y., Wu, Y. X., Wu, Y. H., Xiong, M. C., and Pan, Q. (2024). Adhesion of silicate impact melts on impact glasses of Chang'e-5 regolith. *J. Geophys. Res.: Planets, 129*(12). https://doi.org/10.1029/2024je008777

Yang, W., Chen, Y., Wang, H., Tian, H. C., Hui, H. J., Xiao, Z. Y., Wu, S. T., Zhang, D., Zhou, Q., … Wu, F. Y. (2022). Geochemistry of impact glasses in the Chang'e-5 regolith: Constraints on impact melting and the petrogenesis of local basalt. *Geochim. Cosmochim. Acta*, *335*, 183–196. https://doi.org/10.1016/j.gca.2022.08.030

Zeigler, R. A., Korotev, R. L., Jolliff, B. L., Haskin, L. A., and Floss, C. (2006). The geochemistry and provenance of Apollo 16 mafic glasses. *Geochim. Cosmochim. Acta*, *70*(24), 6050–6067. https://doi.org/10.1016/j.gca.2006.08.040

Zellner, N. E. B., Spudis, P. D., Delano, J. W., and Whittet, D. C. B. (2002). Impact glasses from the Apollo 14 landing site and implications for regional geology. *J. Geophys. Res.: Planets, 107*(E11), 12-1–12-13. https://doi.org/10.1029/2001je001800

Zellner, N. E. B. (2019). Lunar impact glasses: probing the moon's surface and constraining its impact history. *J. Geophys. Res.: Planets*, *124*(11), 2686–2702. https://doi.org/10.1029/2019je006050

Zeng, X. J., Li, X. Y., and Liu, J. Z. (2022). Exotic clasts in Chang'e-5 regolith indicative of unexplored terrane on the Moon. *Nat. Astron.*, *7*(2), 152–159. https://doi.org/10.1038/s41550-022-01840-7

Zhang, L., Zhang, X. B., Yang, M. S., Xiao, X., Qiu, D. G., Yan, J. G., Xiao, L., and Huang, J. (2023). New maps of major oxides and Mg # of the lunar surface from additional geochemical data of Chang'E-5 samples and KAGUYA multiband imager data. *Icarus*, *397*, 115505. https://doi.org/10.1016/j.icarus.2023.115505

Zong, K. Q., Wang, Z. C., Li, J. W., He, Q., Li, Y. H., Becker, H., Zhang, W., Hu, Z. C., He, T., … Liu, Y. (2022). Bulk compositions of the Chang'E-5 lunar soil: Insights into chemical homogeneity, exotic addition, and origin of landing site basalts. *Geochim. Cosmochim. Acta*, *335*, 284–296. https://doi.org/10.1016/j.gca.2022.06.037